BIOMASS AND BIOENERGY 70 (2014) 407–415

Available online at www.sciencedirect.com

ScienceDirect

http://www.elsevier.com/locate/biombioe

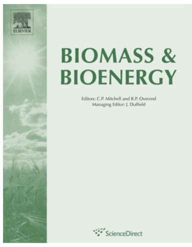

Mild pyrolysis of fast-growing wood species (Caribbean pine and Rose gum): Dimensional changes predicted by the global mass loss

Giana Almeida [a,*], *Diego V.B. Santos* [b], *Patrick Perré* [c]

[a] *UMR 1145, AgroParisTech, INRA, F91305 Massy, France*

[b] *USP (University of São Paulo), ESALQ ("Luiz de Queiroz" College of Agriculture), LQCE (Laboratory of Chemistry, Cellulose and Energy), Piracicaba, Brazil*

[c] *Ecole Centrale Paris, LGPM, Grande Voie des Vignes, 92 290 Châtenay-Malabry, France*

ARTICLE INFO

Article history:
Received 28 March 2014
Received in revised form
21 July 2014
Accepted 26 July 2014
Available online 21 August 2014

Keywords:
Biomass
Eucalyptus grandis
Mass loss
Pinus caribaea var *hondurensis*
Predictive model
Transversal shrinkage

ABSTRACT

Dimensional changes of Caribbean pine and Rose gum (eucalyptus) were continuously measured during mild pyrolysis (heat treatment) with a dynamic mechanical analyzer (DMA) in creep mode with a negligible force. Mass loss was measured on matched samples by thermo-gravimetric analysis (TGA). All experiments were carried out at 220 °C (air and nitrogen), 250 and 280 °C (nitrogen) with a residence time up to 10 h. Eucalyptus exhibits a greater shrinkage and mass loss than pine. By normalizing the shrinkage (heat treatment shrinkage divided by total hygroscopic shrinkage), one single master curve is obtained per species, whatever the heat treatment conditions (temperature, nature of gas) and material direction. For each species, a unique expression is proposed to predict the dimensional changes due to mild pyrolysis as a function of mass loss and total hygroscopic shrinkage. The ability to predict heat treatment shrinkage is useful from industrial perspective (density prediction, change in bed thickness, modeling tools).

© 2014 Elsevier Ltd. All rights reserved.

1. Introduction

Mild pyrolysis, also called "heat treatment" or "torrefaction", allows several physico-mechanical properties of lignocellulosic materials to be modified. During this process, the product is exposed to temperature levels in the range of 200 °C–300 °C under inert atmosphere. The final product is intermediate between wood and charcoal, and exhibits certain technological advantages when compared to the original material such as reduced hygroscopicity, dimensional stabilization, increased durability [1–4]. These changes are due to irreversible modifications in the macromolecular organization. Thermal degradation of hemicelluloses and amorphous cellulose together with condensation of lignins are the most remarkable chemical changes [5–7]. The application of mild pyrolysis is also recommended as a pre-treatment of biomass prior to gasification, as it increases the energy density and the grindability of the treated material [8–13].

Eucalyptus and pine are the most representative species in planted forest areas in Brazil, with over 15,000 and 50,000 km^2 of planted area, respectively [14]. Both are fast-growing species and are intensively used in several industrial domains, such as sawmills, fiberboard production, charcoal for "green" iron, pulp and paper [14]. Also, these planted forests produces a large amount of residues, which can be a widely source of

---

* *Corresponding author*. AgroParisTech, Avenue des Olympiades, F91305 Massy, France.
E-mail addresses: giana.almeida@agroparistech.fr (G. Almeida), patrick.perre@ecp.fr (P. Perré).

http://dx.doi.org/10.1016/j.biombioe.2014.07.028

0961-9534/© 2014 Elsevier Ltd. All rights reserved.

biomass. Several works demonstrate the benefits of applying heat treatment to improve technological properties of fast-growing species [15,10,16].

Technological modifications of wood caused by heat treatment have been investigated since the beginning of the 20th century [17,18]. Among other alterations, it is well known that this process induces dimensional changes (shrinkage), but the majority of studies just measured sample dimensions before and after the heat process. Indeed, works that monitored dimensional changes during the process were focused on charcoal production, thus applying temperature levels higher than 300 °C. For example, Davidsson and Pettersson [19] monitored through a video camera the size changes of birch wood during rapid pyrolysis (350–900 °C, time < 1400 s). Yet, due to the magnitude (up to several times the hygroscopic shrinkage) these dimensional changes have significant impacts, either during the process itself (stress field in large particles, change in thick bed height, change in bed porosity, change in characteristic diffusion time) or to the final product (density, checks, mechanical resistance).

The main purpose of the present study is i) to evaluate the dimensional changes of fast-growing wood species during heat treatment (temperature < 300 °C) using a reliable experimental protocol, and ii) to propose simple mathematical expressions able to predict heat treatment shrinkage as a function of mass loss and hygroscopic shrinkage. This synthetic information will be useful for all questions where the density or the mechanical quality of the final product matters. For example, these expressions can be useful either to assess the complete transformation chain to optimize the heat treatment process to address practical problems or more likely to be implanted in predictive models including ones at industrial scale [20].

2. Materials and methods

2.1. Material selection and preparation

2.1.1. Sampling of vegetal material

Samples were selected from an eleven-year-old Caribbean pine (*Pinus caribaea* var *hondurensis*) and a seven-year-old Rose gum (*Eucalyptus grandis*) commercial plantation located at Lençóis Paulista, São Paulo, Brazil (Lat. 22°35′ S, Long. 48°48′ W). This study was focused to the valorization of forest residues. Therefore, for both species, only the top portion of the trees, mainly composed of juvenile wood, was selected. The dimensions of the collected pieces were 6 cm (diameter) and 40 cm (length). Pieces were gently dried at room temperature until samples preparation. The bark was removed just before samples preparation. The average basic wood density (oven-dry mass to green volume) was 430 kg m^{-3} (coefficient of variation of 4.9%) for Caribbean pine and 390 kg m^{-3} (coefficient of variation of 6.2%) for Rose gum.

2.1.2. Choice of samples dimensions based on moisture and thermal diffusion

To obtain relevant results, the sample temperature has to be as uniform as possible and should follow the furnace temperature as closely as possible. Both constraints can be fulfilled by reducing the sample size, yet keeping a sample long enough to ensure the accuracy of the shrinkage measurement. This is why the smallest dimension, the sample thickness, was always along the longitudinal dimension. In addition, to obtain the same time constant, a thickness of 2 mm was chosen for both dimensional (DMA) and mass loss (TGA) measurements. Based on classical results for transient diffusion inside the sample, the thermal time constant τ reads as [21]:

$$\tau = \frac{h^2 \rho c_p}{\lambda} (s) \tag{1}$$

where h is the half-thickness of the sample (m), ρ is the wood density (kg m^3), c_p is the specific heat capacity of wood (J kg^{-1} K^{-1}) and λ is the thermal conductivity of wood (J s^{-1} m^{-1} K^{-1}).

Using typical values for dry wood ($\rho = 500$ kg m^3, $c_p = 1250$ J kg^{-1} K^{-1} and $\lambda = 0.15$ W m^{-1} K^{-1}) and with a total thickness of 2 mm, the time constant τ is less than 5 s. This value is very small compared to the treatment duration ensuring a uniform treatment throughout the section.

As the initial stage of our protocol is devoted to the determination of the hygroscopic shrinkage, the moisture content gradient rather than the temperature gradient matters during this phase. In principle, an order of magnitude of the hydric time constant could be determined by the analog of equation (1) for transient mass diffusion. Keeping in mind that, in wood, kinetics of moisture diffusion is much longer than thermal diffusion, it becomes obvious that the moisture gradient is likely to be important in the sample during the drying phase. A rigorous analysis of this period is however complex, as many phenomena are involved during this period: coupled heat and mass transfer via the latent heat of evaporation, thermal activation of mass diffusion due to the temperature level, competition between internal and external transfers (boundary layer), both in terms of heat and mass transfer.

To address this difficulty, the comprehensive computational model of coupled heat and mass transfer known as *TransPore* [22,23] was used to quantify these coupling phenomena. We perform a simulation in the case of pine, the less favorable species in terms of permeability, using the actual size of the sample, the temperature schedule defined by our protocol and an external heat transfer coefficient of 25 W m^{-2} K^{-1}. As expected, we have obtained negligible temperature differences during the heat treatment regime: in spite of the exothermic and endothermic reactions, all temperatures, gas, sample surface and sample core, are within 0.1 °C throughout the treatment plateau. During the rapid temperature increase, the surface temperature is one degree below the gas temperature and we have obtained a temperature difference between surface and core of less than 0.4 °C. Unfortunately, as expected due to the hydric time constant, the situation is not as good during the drying phase. Due to evaporation, the sample temperature remains significantly lower than the gas temperature. For example, at 15 min, 5 min after the beginning of the 100 °C-plateau, the sample temperatures are equal to 70 °C and 54 °C, respectively, for surface and core. This temperature gradient corresponds to a time delay between surface and core in terms of moisture content:

the surface reaches the hygroscopic domain after 10 min, against 16 min for the core. A maximum difference of c.a. 10% of bound water content between core and surface is observed during this transient state. Therefore, it is not possible to consider the MC field to be uniform during this period. Consequently, it is not reasonable to analyze the kinetics of the hygroscopic shrinkage: instead, we just computed the total hygroscopic shrinkage, using the fully saturated length and the oven-dry length.

This MC gradient is also likely to generate internal checking, but certainly to a limited extend. Due to the balance of the stress field within the sample, a maximum difference of 10% would turn into a difference of ca. 5% between the average MC and the surface MC. Together with the viscoelastic and mechanosorptive creeps, likely to produce a huge stress relaxation at this temperature level, checking is certainly limited at the very surface of the sample. Hygroscopic shrinkages obtained in this work are in good agreement with the literature (Section 3.1), which confirms the validity of this protocol.

2.1.3. *Samples dimensions for mass and dimensional measurements*

For dimensional measurements along one particular direction, the sample has to be long enough to allow the coupling due to the Poisson's effect close to the clamps to be neglected. For that purpose, sticks coming from the same wood piece and having a transversal section of 30 mm (R or T) × 5 mm (R or T) were cut using a circular saw. From these sticks, the final 2-mm thick samples were cut using a precision diamond wire saw. The final dimensions of radial samples were 30 × 5 × 2 mm (R, T, L), and those of tangential samples were 30 × 5 × 2 mm (T, R, L).

The samples used to monitor the mass loss were prepared following the same methodology. Matched samples were taken next to the samples used for dimensional changes along the longitudinal direction. This allows the effect of wood variability to be reduced as much as possible. However, due to the size limitation of the TGA device used in this case, the samples were shortened using the micro-saw, keeping their middle part, to obtain matched radial samples of 5 × 5 × 2 mm (R, T, L) and matched tangential samples of 5 × 5 × 2 mm (T, R, L).

To be able to determine the hygroscopic shrinkage prior to the heat treatment phase, the samples have to be saturated without any degradation. The following protocol was applied: air-dried samples were placed over distilled water in a desiccator for at least 2 days; they were then submerged in water at room temperature for 2 days and, finally, the samples were kept submerged in a vacuum desiccator with several vacuum cycles for 24 h. Once saturated (above the fiber saturation point), samples were kept under distillated water and stored in a refrigerator until experiments. Just before the tests, the samples were weighed using an analytical balance and saturated dimensions were measured using a micrometer.

2.2. *Experimental protocol*

2.2.1. *Dimensional variation*

The dimensional tests were performed on a *TA Instruments® DMA 2980* system set in creep mode using the tension film clamp. To measure the dimensional changes of unloaded samples ("free" deformation), the smallest tensile load allowed by the equipment (10^{-3} N) was applied to the sample throughout the test. This represents a tensile stress level of 100 Pa, which is really negligible.

As soon as the DMA test starts, the furnace temperature rises and the displacement sensor of the equipment measures continuously the variations in sample length. Different information can be obtained from this test: i) total hygroscopic shrinkage caused by removal of bound water (hygroscopic shrinkage), and ii) shrinkage during the heat treatment process.

The partial hygroscopic shrinkage and the total hygroscopic shrinkage are calculated as follows:

$$\beta^k = \frac{L_H^k - L_0^k}{L_0^k} \quad \text{and} \quad \beta_{\text{tot}}^k = \frac{L_{\text{sat}}^k - L_0^k}{L_0^k} \tag{2}$$

where β^k is the hygroscopic shrinkage, β_{tot}^k the total hygroscopic shrinkage, L_H^k the actual length of the sample in the hygroscopic domain, L_0^k the length at the end of the plateau at 100 °C, L_{sat}^k the length at saturated conditions and k the measurement direction (T or R).

$$\beta_{\text{HT}}^k = \frac{L_0^k - L_{\text{HT}}^k}{L_0^k} \tag{3}$$

where β_{HT}^k is the dimensional shrinkage during the heat treatment, L_{HT}^k, the actual length of the sample during the heat treatment, L_0^k, the length at the end of the plateau at 100 °C and k, the measurement direction (T or R).

Blank tests were conducted to correct the raw data by the expansion of the support due to thermal dilatation. These tests were conducted using Invar (from Good Fellow Cambridge Limited). Invar is an iron (64%) and nickel (36%) alloy presenting a zero expansion coefficient. Blank tests were conducted in duplicate at 220 °C (air), at 250 °C (nitrogen) and at 280 °C (nitrogen), using the same protocol and same sample length as that used for heat treatment. Results show that the thermal dilatation of the device corresponds to a sample expansion of 0.42% for the highest temperature level (280 °C). Even if the value is low, compared to sample shrinkage, observed during tests, the blank tests were used to correct the raw data of all tests.

2.2.2. *Mass loss*

All mass loss tests were performed with a thermogravimetric analyzer (*TGA/DSC 1, Mettler Toledo® system*).

In the case of TGA tests, the initial sample mass is weighted by the balance assembly at room temperature and then, as the furnace temperature rises, the change in sample mass is continuously recorded. Two pieces of information were obtained from this test: moisture content during the hygroscopic domain and mass loss during heat treatment.

$$\text{MC} = \frac{M_H - M_0}{M_0} \tag{4}$$

where MC is the moisture content, M_H is the actual mass of the sample in the hygroscopic domain (g) and M_0 is the mass at the end of the plateau at 100 °C (g).

$$ML = \frac{M_0 - M_{HT}}{M_0} \quad (5)$$

where ML is the mass loss due to heat treatment, M_{HT} is the actual mass during the heat treatment (g) and M_0 is the mass at the end of the plateau at 100 °C (g).

2.2.3. *Temperature schedule*

All tests were carried out at 220 °C (under nitrogen and atmospheric conditions), and 250 and 280 °C (under inert atmosphere). As all experimental data are continuously recorded (time, mass, dimension, sample temperature), such a long residence time allows us to extensively study the wood degradation behavior, from short to long residence times. Runs were done following the same schedule, which is composed of an initial heating stage from room temperature to 100 °C, held there for 60 min to obtain equilibrium at this temperature. Then the sample is heated to the maximum torrefaction temperature (220, 250 or 280 °C) and held at this value for 570 min, and finally cooled to room temperature. Both heating and cooling rates were set at 10 K min^{-1}. To verify the reproducibility of our data, duplicates were performed on matched samples and very similar results were always obtained.

2.2.4. *Microscopic observation*

To go further into the interpretation of the mechanisms behind dimensional variation due to heat treatment, anatomical observations were made on matched samples. One face of these samples was prepared using a slide microtome with disposable blades. The native sample was first observed using an ESEM microscope (Environmental Scanning Electronic Microscopy, FEI Quanta 200). To be able to find the same zone after heat treatment, successive images were grabbed at increasing magnification. Thereafter, the sample was heat-treated using the DMA furnace and the same schedule as for the other tests. Thanks to the series of images, it was possible to find the same zone and magnify it. To be able to quantitatively compare the image dimensions, the same experimental conditions inside the ESEM chamber were applied for all image acquisition (detector: secondary electrons; mode: low vacuum; pressure: 133 Pa; spot size: 5).

3. Results and discussion

3.1. *Thermogravimetric and dimensional experimental data*

Fig. 1 presents an example of the full set of raw data obtained during TGA and DMA tests. The curves typically present two stages. The first concerns water removal. As the sample is initially saturated, a large amount of free water was present in the sample, which explains the huge loss of mass over a short time. Notice that only the removal of bound water produces dimensional changes. This explains why the mass decreases rapidly even at very short times, whereas the shrinkage curves present an initial slope close to zero. As previously mentioned, it is not possible to consider the MC field to be uniform during this period. Therefore, the curve shape will

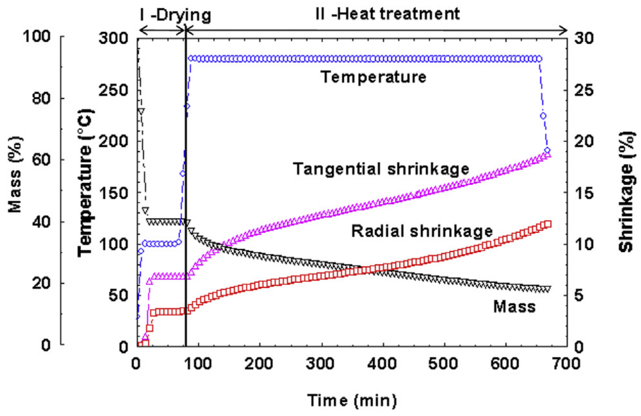

Fig. 1 – Example of a full set of experimental data (Caribbean pine, 280 °C). (I) Heating at 100 °C to remove moisture and measure radial/tangential hygroscopic shrinkages. (II) Heating at 280 °C with mass loss and radial/tangential shrinkages caused by mild pyrolysis. Mass (%) is the percentage of initial mass.

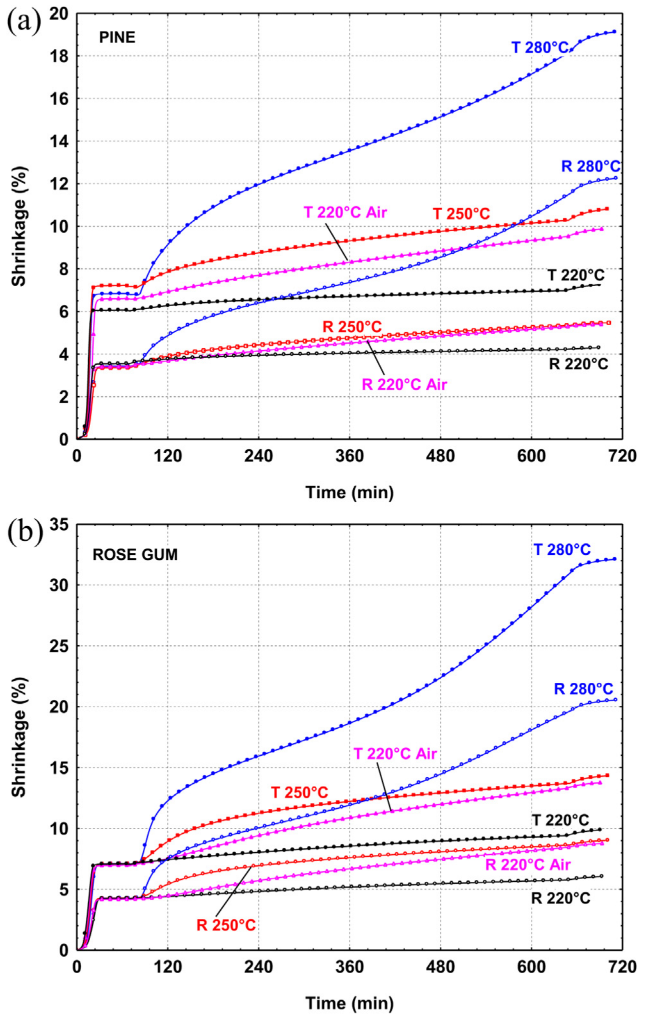

Fig. 2 – Radial and tangential shrinkage measured versus time: the full set of data obtained for the Caribbean pine (2a) and Rose gum (eucalyptus) (2b) for treatments at 220 °C (air and N_2), 250 °C (N_2) and 280 °C (N_2).

not be analyzed further during this drying phase and only the total shrinkage from saturated stage (initial length) to 0% MC (at the end of the 100 °C plateau) will be mentioned hereafter as hygroscopic shrinkage (Fig. 2). The second stage starts basically at the beginning of the heat treatment plateau (280 °C in the figure), as the high heating rate used in this work allows the sample to attain the plateau temperature with very little thermal attack. From that time, changes of mass and dimensions are caused by thermal degradation of lignocellulosic matter.

Results obtained for all tests are summarized in Table 1. As expected, the mass loss caused by heat treatment increased with the treatment temperature and residence time, both for eucalyptus and pine. This table clearly indicates that, at any temperature level and residence time (except some low very values obtained at short times), eucalyptus depicts higher mass loss and dimensional change levels than pine. This fact confirms previous findings regarding the thermal resilience of cell wall components. At first, it is well known that, for moderate treatments, the degradation of hemicelluloses explains a large part of mass loss [24,25,6]. Kamdem et al. [3] showed that hardwood hemicelluloses are more sensitive to thermal degradation. In addition, the native lignins of conifers are essentially constituted of guaiacyl (G) units together with a low proportion of p-hydroxyphenyl (H) units. Along with the G units and traces of H units, the lignins of hardwoods species constitute syringyl (S) units. The proportion of resistant bonds (condensed linkages) in native lignins increases with the frequency of G and H units whereas S units are mostly involved in β-O-4 linkages. Consequently, hardwood lignins are more sensitive to heat treatment than those of softwoods [26,7].

In agreement with literature data [27], Table 1 confirms that, for both species, the hygroscopic shrinkage in tangential direction is roughly twice the radial one. Early works relate the influence of ray cells, which partially inhibit the free wood shrinkage in the radial direction, as one cause of the transversal anisotropy of wood [28]. As the specimens studied here are mostly composed of juvenile wood, it is not surprising to

Table 1 – Results of dimensional shrinkage and mass loss at several mild pyrolysis conditions (time, temperature, atmosphere) for Caribbean pine and Rose gum (eucalyptus).

Species	Condition		Mass loss (%) (standard deviation)[b]	Shrinkage (%) (Normalized shrinkage)[c]	
				Radial	Tangential
Caribbean pine	Hygroscopic domain[a]		–	3.44	6.69
	Mild pyrolysis	220 °C air, 10′	1.07 (0.07)	0.02 (0.01)	0.07 (0.01)
		220 °C air, 60′	3.93 (0.44)	0.25 (0.07)	0.51 (0.08)
		220 °C air, 300′	11.50 (1.61)	1.09 (0.32)	1.92 (0.29)
		220 °C air, 570′	17.30 (2.33)	1.85 (0.54)	3.16 (0.47)
		220 °C N2, 10′	0.68 (0.04)	0.02 (0.01)	0.05 (0.01)
		220 °C N2, 60′	1.96 (0.06)	0.15 (0.04)	0.26 (0.04)
		220 °C N2, 300′	4.38 (0.04)	0.40 (0.12)	0.68 (0.10)
		220 °C N2, 570′	5.99 (0.01)	0.59 (0.17)	0.98 (0.15)
		250 °C N2, 10′	2.46 (0.01)	0.12 (0.03)	0.22 0.03)
		250 °C N2, 60′	6.64 (0.13)	0.54 (0.16)	0.98 (0.15)
		250 °C N2, 300′	14.58 (0.43)	1.34 (0.39)	2.40 (0.36)
		250 °C N2, 570′	19.44 (0.71)	1.91 (0.55)	3.42 (0.51)
		280 °C N2, 10′	6.70 (0.31)	0.50 (0.15)	0.91 (0.14)
		280 °C N2, 60′	17.86 (0.49)	1.69 (0.49)	3.23 (0.48)
		280 °C N2, 300′	35.94 (0.80)	4.01 (1.16)	7.37 (1.10)
		280 °C N2, 570′	51.70 (0.96)	8.17 (2.37)	12.2 (1.83)
Rose gum	Hygroscopic domain		–	4.38	7.08
	Mild pyrolysis	220 °C air, 10′	0.75 (0.07)	0.01 (0.00)	0.09 (0.01)
		220 °C air, 60′	4.43 (0.57)	0.47 (0.11)	0.79 (0.11)
		220 °C air, 300′	13.10 (1.48)	2.71 (0.62)	4.28 (0.60)
		220 °C air, 570′	18.70 (2.14)	4.48 (1.02)	6.77 (0.96)
		220 °C N2, 10′	0.60 (0.11)	0.01 (0.00)	0.07 (0.01)
		220 °C N2, 60′	2.30 (0.36)	0.19 (0.04)	0.39 (0.06)
		220 °C N2, 300′	7.04 (0.98)	0.98 (0.22)	1.55 (0.22)
		220 °C N2, 570′	9.59 (1.29)	1.59 (0.36)	2.46 (0.35)
		250 °C N2, 10′	3.91 (0.23)	0.22 (0.05)	0.41 (0.06)
		250 °C N2, 60′	10.97 (0.41)	1.64 (0.37)	2.58 (0.36)
		250 °C N2, 300′	18.45 (0.17)	3.52 (0.80)	5.52 (0.78)
		250 °C N2, 570′	22.72 (0.37)	4.55 (1.04)	7.04 (0.99)
		280 °C N2, 10′	9.66 (0.23)	1.48 (0.34)	2.46 (0.35)
		280 °C N2, 60′	18.82 (0.28)	4.01 (0.92)	6.35 (0.90)
		280 °C N2, 300′	40.02 (1.96)	8.28 (1.89)	12.7 (1.80)
		280 °C N2, 570′	62.31 (0.49)	16.1 (3.7)	25.7 (3.6)

[a] Hygroscopic domain: shrinkage values from FSP (fiber saturation point) to 0% MC (moisture content).
[b] Standard deviation of mass loss (between parentheses, in italic).
[c] Normalized shrinkage: heat treatment shrinkage divided by the total hygroscopic shrinkage.

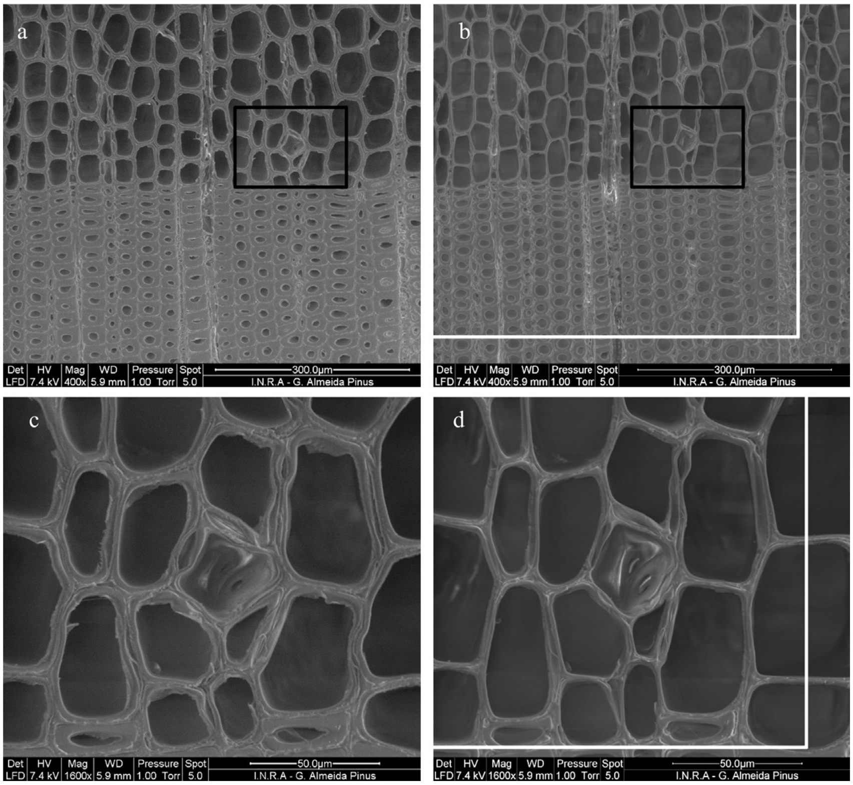
a
Det HV Mag WD Pressure Spot
LFD 7.4 kV 400x 5.9 mm 1.00 Torr 5.0
300.0µm
I.N.R.A - G. Almeida Pinus
b
Det HV Mag WD Pressure Spot
LFD 7.4 kV 400x 5.9 mm 1.00 Torr 5.0
300.0µm
I.N.R.A - G. Almeida Pinus
c
Det HV Mag WD Pressure Spot
LFD 7.4 kV 1600x 5.9 mm 1.00 Torr 5.0
50.0µm
I.N.R.A - G. Almeida Pinus
d
Det HV Mag WD Pressure Spot
LFD 7.4 kV 1600x 5.9 mm 1.00 Torr 5.0
50.0µm
I.N.R.A - G. Almeida Pinus

Fig. 3 – ESEM micrographs of a transversal section of the Caribbean pine. (3a) General view of untreated sample. (3b) General view of heat treated sample at 280 °C, 570 min (3c) Earlywood tracheids' cell wall of untreated sample (black square zone on the general view). (3d) Earlywood tracheids' cell wall of heat treated sample (black square zone on the general view). White squares show the image dimension before mild pyrolysis.

observe values that are rather low for transverse shrinkage. Indeed, the S_2 layer of juvenile wood has higher microfibril angle compared to normal wood, which is known to lower transversal shrinkage and increase longitudinal shrinkage [29].

In the analysis of the dimension shrinkage induced by thermal degradation, it is interesting to notice the same shrinkage anisotropy ($T \approx 1/2R$) as that observed for hygroscopic shrinkage (Table 1). Thus, in certain aspects, the dimensional changes due to thermal degradation obey the same rules as those induced by bound water adsorption/desorption. Nevertheless, it is important to highlight that the hygroscopic shrinkage is reversible whereas the shrinkage caused by thermal degradation is irreversible. In addition, it is worth keeping in mind that this permanent degradation lowers the amount of bound water in heat-treated wood, hence the hygroscopic shrinkage of the new material [4].

Among important results, Table 1 tells us that the higher mass loss of eucalyptus, due to easier chemical degradation of hardwood, turns into higher dimensional changes, not only in

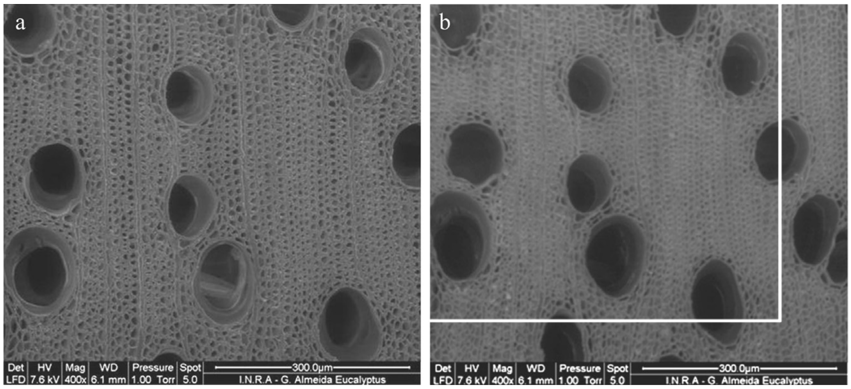
a
Det HV Mag WD Pressure Spot
LFD 7.6 kV 400x 6.1 mm 1.00 Torr 5.0
300.0µm
I.N.R.A - G. Almeida Eucalyptus
b
Det HV Mag WD Pressure Spot
LFD 7.6 kV 400x 6.1 mm 1.00 Torr 5.0
300.0µm
I.N.R.A - G. Almeida Eucalyptus

Fig. 4 – ESEM micrographs of a transversal section of Rose gum (eucalyptus). (4a) Untreated sample. (4b) Heat treated at 280 °C, 570 min. White square shows the image dimension before mild pyrolysis.

absolute values, but also in proportion of the hygroscopic shrinkage.

ESEM images of native and heat-treated samples can be observed in Figs. 3 and 4. For each couple of images (before and after treatment), using the same imaging parameters insures that the field of view is the same. This allows the shrinkage of wood cells caused by mild pyrolysis to be perfectly observed: a larger part of the sample can be observed after treatment. To ease the observation, the exact zone of the native sample was highlighted on each heat-treated sample by a white rectangle (Figs. 3b, d and 4b). These images clearly confirm that the tangential deformation is larger than the radial deformation. In addition, one can distinguish slight changes in the cellular shape: changes in tracheid's angles become more “rectangular” in pine and in vessel's shape in eucalyptus are flattened along the tangential direction. The drastic reduction of the cell-wall thickness due to molecular degradation (zoom in Fig. 3) is certainly the main reason for macroscopic shrinkage and resembles, in this sense, that which can be observed in hygroscopic shrinkage [30].

A distinct effect of treatment atmosphere at the same temperature (220 °C) can be observed in both radial and tangential directions for both species. Table 1 shows that thermal treatment under air atmosphere induces higher dimensional shrinkage than under nitrogen (after 570 min of treatment, β_{Tair} is about twice $\beta_{\mathrm{Tnitrogen}}$ for eucalyptus and almost three times that of pine). The oxygen present in the air produces oxidation and the chemical changes induced on wood are more intense, so the decomposition of the hemicelluloses and cellulose components is enhanced [31]. Notice that the same trend is observed for mass loss: the change of gas does not break the relation between shrinkage and mass loss.

3.2. *Mass loss as indicator of dimensional changes*

In previous works, it was shown that the mass loss due to heat treatment is a synthetic variable able to predict the alterations of several properties [10,11]. To further test this conjecture, the radial and tangential shrinkages were plotted as a function of mass loss for pine and eucalyptus. In addition, as heat treatment and hygroscopic shrinkages obey similar rules, the heat treatment shrinkage was normalized by dividing its values by the hygroscopic shrinkage (for each sample, the division was made by the hygroscopic shrinkage of the same sample).

The plotted curves (Figs. 5 and 6) are spectacular: a unique curve clearly appears for each species, whatever the material direction and the treatment conditions, up to more than 30% of mass loss. This value includes all treatments tested in this work even for the longest residence times, except the treatment at 280 °C, over 3–4 h. For the most severe conditions (280 °C), the master curve eventually fails above c.a. 40% of mass loss, with a normalized shrinkage becoming larger for the radial test.

Mathematical expressions were fitted on the two master curves to predict the heat treatment shrinkage (Table 2). All expressions proposed here are forced to the origin, as it makes sense to have no dimensional change without mass loss. The curve obtained for pine is almost linear ($R^2 = 0.977$). However, the initial slope of the curve is slightly smaller than the remaining part. This is why we propose two expressions for pine: a power law and a simple linear expression. Notice that the difference of accuracy between these two expressions is not so important, so we would recommend the simpler expression in the case of pine. It is worth noticing that the normalized value reaches 1 for about 30% of mass loss: this means that 30% of mass loss due to heat treatment induces

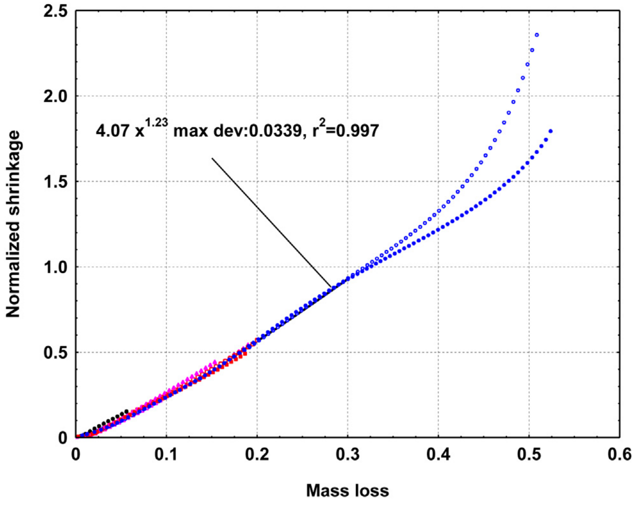

Fig. 5 – Master curve obtained for the Caribbean pine: normalized shrinkage (heat treatment shrinkage divided by the total hygroscopic shrinkage) as a function of mass loss (open marks = radial tests, plain marks = tangential tests). The normalization works perfectly until 35% of mass loss. In addition, in the case of pine, the master curve is almost perfectly linear up to this value.

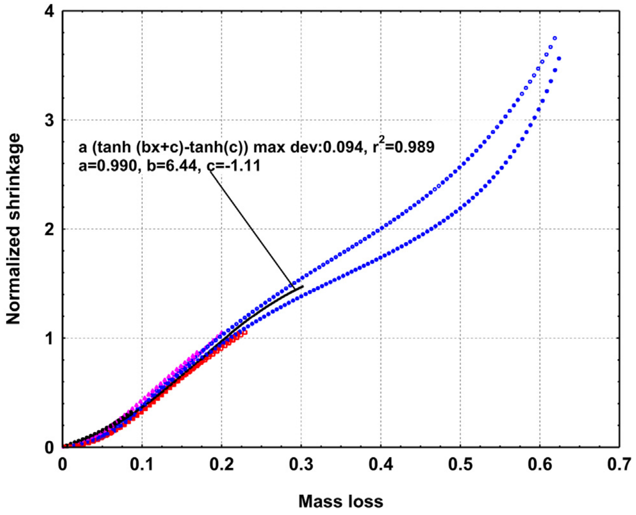

Fig. 6 – Master curve obtained for Rose gum (eucalyptus): normalized shrinkage (heat treatment shrinkage divided by the total hygroscopic shrinkage) as a function of mass loss (open marks = radial tests, plain marks = tangential tests). The normalization works nicely until 30% of mass loss. In the case of eucalyptus, an S-shaped master curve is obtained between 0% and 30% of mass loss.

Table 2 – Expressions proposed for the Caribbean pine and Rose gum (eucalyptus) to predict normalized shrinkage from mass loss. For the sake of simplicity, a simple linear expression is proposed for both species, even though this linear relationship is not so good for eucalyptus. All expressions are forced to the origin (no dimensional change for a mass loss equal to zero).

	Expressions proposed to predict the normalized shrinkage[a]	Maximum error	R^2
Caribbean pine	$\frac{\beta^k_{\mathrm{HT}}}{\beta^k_{\mathrm{tot}}} = 4.07\ \mathrm{ML}^{1.23}$	0.034	0.997
	$\frac{\beta^k_{\mathrm{HT}}}{\beta^k_{\mathrm{tot}}} = 2.78\ \mathrm{ML}$	0.090	0.977
Rose gum	$\frac{\beta^k_{\mathrm{HT}}}{\beta^k_{\mathrm{tot}}} = 4a\{\tanh(b\mathrm{ML} + c) - \tanh(c)\}$	0.094	0.989
	$a = 0.990;\ b = 6.44\ c = -1.11$ $\frac{\beta^k_{\mathrm{HT}}}{\beta^k_{\mathrm{tot}}} = 4.58\ \mathrm{ML}$	0.162	0.955

$\beta^k_{\mathrm{HT}}/\beta^k_{\mathrm{tot}}$ is the normalized shrinkage (heat treatment shrinkage divided by the total hygroscopic shrinkage) and k is the material direction (radial or tangential).

[a] Expressions valid up to 30% of mass loss for all conditions tested in the present work.

the same dimensional change as a change of 30% of bound water (from FSP to 0% MC).

An S-shape curve is obtained for eucalyptus between 0 and 30% of mass loss. This is why we fitted the curve using a hyperbolic tangent (Table 2). For eucalyptus, the accuracy is not as good as for pine, but the maximum error remains less than 10%, which means that the shrinkage induced by heat treatment can be predicted with a maximum error below one tenth of the hygroscopic shrinkage. Keeping in mind that this is valid whatever the treatment conditions and the material direction, this is rather good. The hygroscopic shrinkage itself is usually not known with a better accuracy. For a very simple approach, we also propose a linear expression for eucalyptus, although its maximum error reaches 16% (last line of Table 2). The slope of this linear expression (4.58) is much higher that the one obtained for pine (2.78). This reflects a very strong experimental fact: for eucalyptus, a mass loss of 30% produces a normalized heat treatment of c.a. 1.5, the total hygroscopic shrinkage, as against 0.9 for pine. Therefore, three reasons explain why the absolute shrinkage due to heat treatment is higher for eucalyptus than for pine:

1) the total hygroscopic shrinkage is higher for eucalyptus,
2) for a certain mass loss, the normalized shrinkage is c.a. 1.6 times greater for eucalyptus,
3) for similar treatment conditions, the mass loss is higher for eucalyptus.

The cumulative effects of these three trends give, for example, a tangential shrinkage equaling 25.7% for eucalyptus (resp. 12.2% for pine) at the end of the treatment at 280 °C and 7.04% for eucalyptus (resp. 3.42% for pine) at the end of the treatment at 250 °C.

The linear shape of the master curve observed for pine can be explained by the anatomical structure of softwood species, which are simpler than that of hardwood species. Indeed, one anatomical element (longitudinal tracheids) represents more than 90% of volume in softwoods. Also, ray elements of softwoods are generally uniseriated and represent less than 5% of wood volume [32].

The case of hardwoods is more complex for at least two reasons: i) as stated above, the higher proportion of the high level of β-O-4 linkages between lignin units, prone to condensation, and ii) a dual-scale porosity of the anatomical structure (fibers and vessels), with differences of chemical composition, hence different kinetics of thermal degradation. The first feature is likely to explain why the normalized shrinkage is higher for eucalyptus while the second one is a possible explanation for the S-shape master curve.

4. Conclusion

Mass loss and dimensional changes of Caribbean pine and Rose gum were continuously measured during mild pyrolysis (heat treatment) using a dynamic mechanical analyzer. The difference of behavior found between these two species was explained by their anatomical and chemical features. Heat treatment shrinkage of eucalyptus was up to four times that of the hygroscopic shrinkage.

By normalizing the shrinkage (heat treatment shrinkage divided by total hygroscopic shrinkage), one single master curve is obtained per species, whatever the heat treatment conditions (temperature, nature of gas) and material direction. The dimensional change due to the heat treatment (or during the treatment) is then predicted as a function of mass loss and total hygroscopic shrinkage. This confirms the particular status of mass loss as synthetic parameter, easy to measure and able to predict the alternation of many other properties [10]. The ability of these functions to predict the heat treatment shrinkage is suitable to help in process design (change in particle volume and bed porosity, checking of large particles), to solve existing industrial issues and/or to supply data to modeling tools.

Acknowledgments

The authors like to thank the late colleague Patrice Marchal (LERFoB/INRA) who gave valuable help in DMA/TGA measurements. The authors would also like to thank Ana Lúcia Piedade Sodero Martins Pincelli and Professor José Otávio Brito (ESALQ/USP) for grateful help in sample collection. This work was financially supported by International Cooperation between Brazil and France (Capes/Cofecub, project 601/08).

REFERENCES

[1] Brito JO. Reflexões sobre qualidade do carvão vegetal para uso siderúrgico. Piracibaca, Brazil: Circular Técnica IPEF; February 1993. p. 6. Report No. 181.

[2] Gohar P, Guyonet R. Development of wood rectification process at the industrial stage. In: Proceedings of the 4th International Symposium on Wood Preservation; 2–4 February 1998; Cannes, France; 1998. p. 173–8.

[3] Kamdem DP, Pizzi A, Jermannaud A. Durability of heat-treated wood. Holz Roh-Werkst 2002;60:1–6.

[4] Almeida G, Brito JO, Perré P. Changes in wood-water relationship due to heat treatment assessed using micro-samples of Eucalyptus. Holzforschung 2009;63:80–8.

[5] Windeisen E, Strobel C, Wegener G. Chemical changes during the production of thermo-treated beech wood. Wood Sci Technol 2007;41:523–36.

[6] Brito JO, Silva FG, Leao M, Almeida G. Chemical composition changes of eucalyptus and pinus woods submitted to heat treatment. Bioresour Technol 2008;99(18):8545–8.

[7] Rousset P, Lapierre C, Pollet B, Quirino W, Perré P. Effect of severe thermal treatment on spruce and beech wood lignins. Ann For Sci 2009;66. 110p1–110p8.

[8] Bergman PCA, Kiel JHA. Torrefaction for biomass upgrading. The Netherlands: ECN; 2005. p. 8. Report ECN-RX–05-180.

[9] Arias B, Pevida C, Fermoso J, Plaza MG, Rubiera F. Influence of torrefaction on the grindability and reactivity of woody biomass. Fuel Process Technol 2008;89(2):169–75.

[10] Almeida G, Brito JO, Perré P. Alterations of energy properties of eucalyptus wood and bark subjected to torrefaction: the potential of mass loss as a synthetic indicator. Bioresour Technol 2010;101(24):9778–84.

[11] Pierre F, Almeida G, Brito JO, Perré P. Influence of torrefaction on some chemical and energy properties of maritime pine and pedunculate oak. BioResources 2011;6(2):1204–18.

[12] Clarke S, Preto F. Biomass Densification for Energy production. Ontario, Canada: Fact sheet order, Ministry of Agriculture, Food and Rural Affairs; June 2011. p. 6. Report No. 11-035 AGDEX 737/120.

[13] Van Essendelft DT, Zhou X, Kang BSJ. Grindability determination of torrefied biomass materials using the hybrid work index. Fuel Process Technol 2013;105:103–11.

[14] ABRAF – Brazilian association of Forest plantation Producers. Yearbook statistical 2013. Base year 2012. Brasilia, Brazil; 2013. p. 148. Available from:, http://www.abraflor.org.br/estatisticas/ABRAF13/ABRAF13_EN.pdf.

[15] Santos AJ. Mechanical behavior of eucalytpus wood modified by heat. Wood Sci Technol 2000;34:39–43.

[16] De Moura LF, Brito JO, Nolasco AM, Uliana LR. Effect of thermal rectification on machinability of *Eucalyptus grandis* and *Pinus caribaea var. hondurensis* woods. Eur J Wood Wood Prod 2011;69:641–8.

[17] Stamm AJ, Hansen LA. Minimizing wood shrinkage and swelling. Effect of heating in various gasses. Ind Eng Chem 1937;29(7):831–3.

[18] Stamm AJ, Burr HK, Kline AA. Staybwood. Heat stabilized wood. Ind Eng Chem 1946;38(6):630–4.

[19] Davidsson KO, Pettersson JBC. Birchwood particles shrinkage during rapid pyrolysis. Fuel Process Technol 2002;81:263–70.

[20] Perré P, Rémond R, Turner IW. A comprehensive dual-scale wood torrefaction model: application to the analysis of thermal run-away in industrial heat treatment processes. Int J Heat Mass Transf 2013;64:838–49.

[21] Bird RB, Stewart WE, Lightfoot EL. Transport phenomena. New York: John Wiley and Sons, Inc.; 1960.

[22] Perré P, Turner IW. Transpore: a generic heat and mass transfer computational model for understanding and visualising the drying of porous media. Dry Technol 1999;17:1273–89.

[23] Turner IW, Rousset P, Rémond R, Perré P. An experimental and theoretical investigation of the thermal treatment of wood in the range 200–260 °C. Int J Heat Mass Transf 2010;53:715–25.

[24] Yildiz S, Gezer ED, Yildiz UC. Mechanical and chemical behavior of spruce wood modified by heat. Build Environ 2006;41:1762–6.

[25] Inari GN, Petrissans M, Gerardin P. Chemical reactivity of heat-treated wood. Wood Sci Technol 2007;41:157–68.

[26] Avat F. Contribution à l'étude des traitements thermiques du bois jusqu'à 300 °C: transformations chimiques et caractérisations physico-chimiques. Ph.D. Thesis. France: Ecole des Mines de Saint-Etienne; 1993.

[27] Kollmann F, Côte WA. Principles of wood science and technology. Solid Woodvol. 1. New York: Springer Verlag; 1968.

[28] Barkas WW. Wood water relationships, VI. The influence of ray cells on the shrinkage of wood. Trans Faraday Soc 1941;37:535–47.

[29] Larson PR, Kretschmann DE, Clark III A, Isebrands JG. Formation and properties of juvenile wood in southern pines: a synopsis. Madison, U.S: Gen. Tech. Rep. Department of Agriculture, Forest Service, Forest Products Laboratory; September 2001. p. 42. FPL-GTR-129.

[30] Almeida G, Huber F, Perré P. Free shrinkage of wood determined at the cellular level using an environmental scanning electron microscope. Rev Maderas 2014;16(2):187–98.

[31] Broström M, Nordin A, Pommer L, Branca C, Di Blasi C. Influence of torrefaction on the devolatilization and oxidation kinetics of wood. J Anal Appl Pyrol 2012;96:100–9.

[32] Panshin AJ, de Zeeuw C. Textbook of wood technology. structure, identification, properties and uses of the commercial woods of the United States and Canada. New York: McGraw-Hill; 1980.